Effect of cutting angles during the micro-groove fabrication process using a non-rigid cutting mechanism

German Herrera-Granados[1,#], Kiwamu Ashida[2,#], Ichiro Ogura[2], Yuichi Okazaki[2], Noboru Morita[1], Hirofumi Hidai[1], Souta Matsusaka[1] and Akira Chiba[1]

1 Graduate School of Engineering, Chiba University, Chiba, Japan
2 Advanced Manufacturing Research Institute, National Institute of Advanced Industrial Science and Technology, Ibaraki, Japan
Corresponding Author / E-mail: german.hg@chiba-u.jp, ashida.k@aist.go.jp, TEL: +81-29-861-7155, FAX: +81-29-861-7201

KEYWORDS : Constant Load Cutting, Micro-Groove Cutting, AFM machining, Diamond Cutting

A non-rigid micro-scale cutting mechanism with a large manufacturing area was recently developed for fabrication of micro-grooves. This mechanism has a diamond tool chip that is attached at the free edge of a cantilever beam, which is used to remove the material. During the cutting process, due to the interaction between the tool and the workpiece, the cantilever beam presents a deformation that is used to implement a force feedback control system, obtaining as result the fabrication of grooves with a constant cutting depth. However, due to its non-rigid property, the forces involved in the cutting process affect this system more significantly that to a conventional machine. The cutting angles (rake, wedge and inclination) affect directly the cutting forces, and for that reason, it was required to observe its effect on this new cutting mechanism. Experimental analysis was realized to determine the best conditions required to improve the quality of the micro-grooves developed with this system.

NOMENCLATURE

CFC = Constant feed cutting
CLC = Constant load cutting
FFBC = Force feedback controller
d_G = Depth of the groove
α = Rake face angle
γ = Flank (or relief) angle
t_0 = Uncut chip thickness
w_0 = Uncut chip width
t_C = Chip thickness
w_C = Chip width
λ = Cutting edge inclination angle
ϕ = Shear plane angle
r_T = Chip thickness ratio
α_t = Effective rake face angle
R = Tool edge radius
θ = Wedge or cutting angle
F_C = Cutting force
A = Area of the cutting cross section
k_m = Specific cutting energy coefficient
C,n = Experimental constants

1. Introduction

In recent years, the development of mechanical components with high precision micro-textured surfaces, such as micro-grooves, is getting increased due to its wide application on different industrial fields; e.g., in the fabrication of optical lenses, prism sheets for LCD panels, surfaces with textures to produce the "lotus effect" to repel water, micro channels for heat exchangers, between others. Nowadays, precision machining with diamond tools has been rapidly growing in the manufacturing of high precision machined parts for advanced industrial applications. The outstanding hardness and crystalline structure of diamond make possible to fabricate diamond cutters with very sharp cutting edges which are necessary for precision machining [1]. Recently, the use of diamond tools for the fabrication of micro-grooves and micro-structures has been increased significantly [2-5]. However, due to the characteristics of the cutting process, ultra precision motion mechanisms and a very strict environmental control are required to obtain the desired

precision in the nano/micro-scale order on the machined work. This is principally because conventional cutting machines set the cutting depth by its feed mechanism (hereinafter referred as Constant Feed Cutting, CFC), so the preciseness of the produced part depends directly on the accuracy of the machine involved in its fabrication (fig. 1a). To give a solution to this issue, a Constant Load Cutting (CLC) mechanism (fig. 1b) was proposed [6-7]. Its operation is based on a similar principle to the one applied on the nano-cutting system using an atomic force microscope (AFM) [8-11], where nano-scratches are made using a sharp tip mounted flexible on a micro-cantilever (fig. 2).

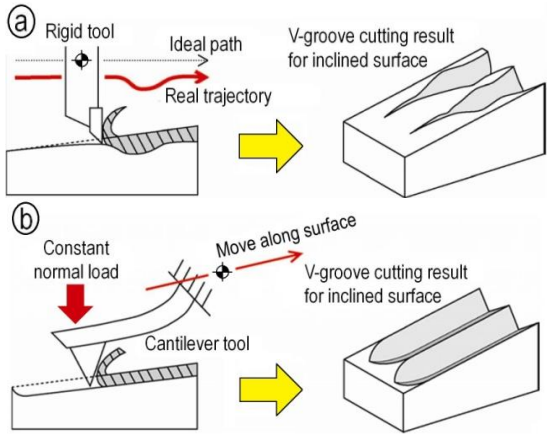

Fig. 1 (a) Constant Feed Cutting (CFC) and (b) Constant Load Cutting (CLC) principles and their results.

Due to the fact that the tool is mounted on a non-rigid mechanism, the most important parameter to be studied in this system is the deformation of the cantilever beam, which is directly related to the cutting forces present on the manufacturing process. Different from conventional CFC mechanisms, parameters such as the cutting direction, the tool geometry and the workpiece material might affect significantly the behavior of this mechanism. Previously [7, 12], basic analysis of the effects of the workpiece material and the cutting direction on this mechanism has been done. In this paper, an experimental analysis is presented to study the effects of the tool geometry on the performance of this system. Prior this analysis, the CLC mechanism and its characteristics are shown.

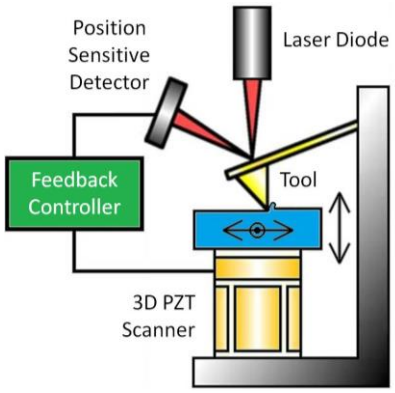

Fig. 2 Nano-cutting using an AFM mechanism

2. Constant load cutting mechanism

2.1 Setup of the CLC mechanism

To apply the CLC principle to develop micro structured surfaces, a novel cutting mechanism has been developed. This system can be divided in two main subsystems: the cutting mechanism and the motion system.

The cutting mechanism consists on a single crystal diamond tool chip that is mounted at the edge of a parallel leaf spring cantilever. When the manufacturing process is performed, the interaction between the tool and the workpiece makes the cantilever to present a flexural deformation. This deformation is necessary to implement a force feedback controller (FFBC), which will control the relative position between the tool and the workpiece (GAP), and therefore, the normal cutting force. The GAP, measured by a capacitive linear displacement sensor, is compared to a reference voltage using a PI controller, and the output is sent to a piezoelectric actuator (PZT) that will expand or retract, depending on the case, in order to maintain constant the deformation of the cantilever. Figure 3 shows a simple diagram of the cutting mechanism developed including the FFBC.

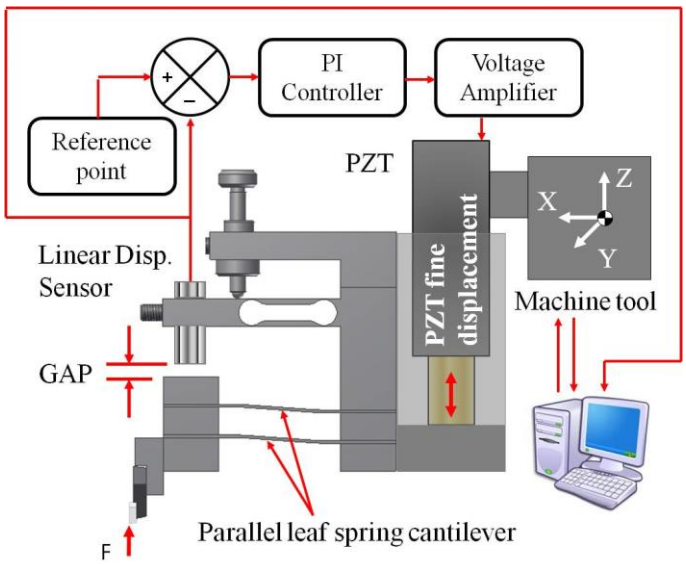

Fig. 3 CLC mechanism with FFBC

The cutting mechanism is mounted on the Z axis of the motion system, which consists on a precision 3 axis numerical control (NC) machine tool, which provides a larger machining area compared to the conventional AFM systems. Figure 4 shows the setup of the system. The control of the NC machine tool is done by a LabVIEW interface, which also collects the data from the cutting experiments.

2.2 Behavior of the CLC mechanism

Figure 5 shows the expected behavior of the CLC mechanism during cutting experiments performed over inclined surfaces, comparing both cases, when the FFBC is active and when it is not active. Table 1 shows the cutting conditions of the

experiments done to confirm such behavior. According to the results, it is possible to conclude that when the FFBC is active, the CLC mechanism can compensate the surface inclination, regardless of the direction, and maintain constant the cutting depth; on the other hand, when the FFBC is not active, the cutting depth will increase or decrease, depending on the direction of the surface inclination (fig. 6) [12].

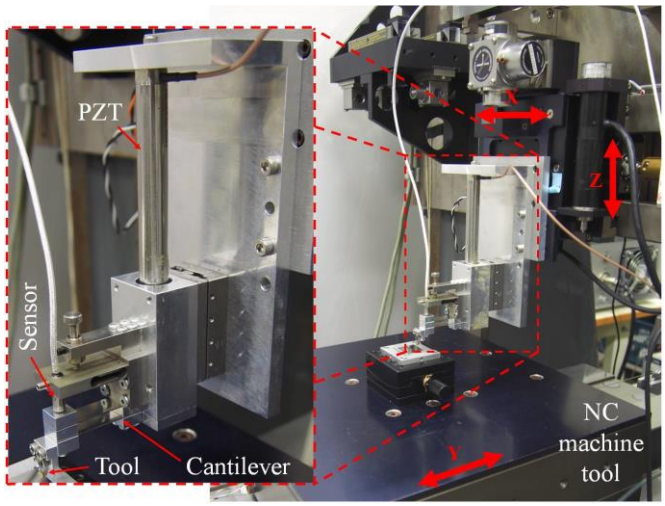

Fig. 4 Setup of the CLC

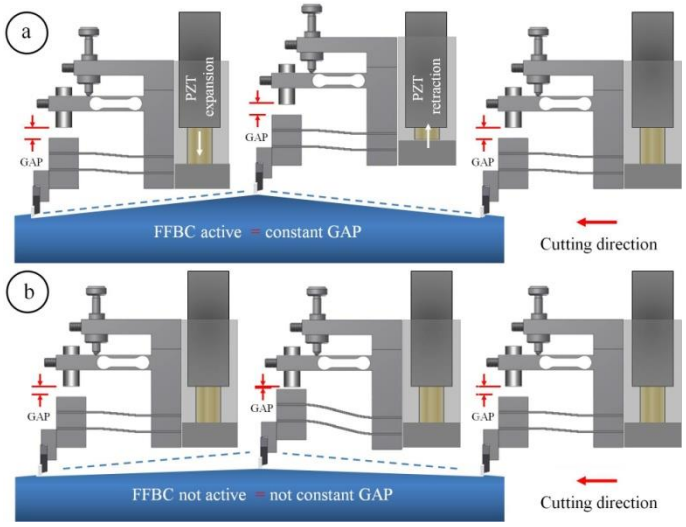

Fig. 5 Schematic of the CLC mechanism behavior when: (a) the FFBC is active and (b) the FFBC is not active

Table 1. Conditions for experiments on inclined surfaces

Workpiece material	Brass (C2801)
Surface inclination	±2 [μm/mm]
Tool material	Single crystal diamond
Tool shape	V-shape, 90° cutting angle
Length of the groove	10 [mm]
Initial indentation	10 [μm] (feed by Z-axis)
Feed rate	6 [mm/min]
Cutting direction	Front cutting
Others	Dry and orthogonal cutting

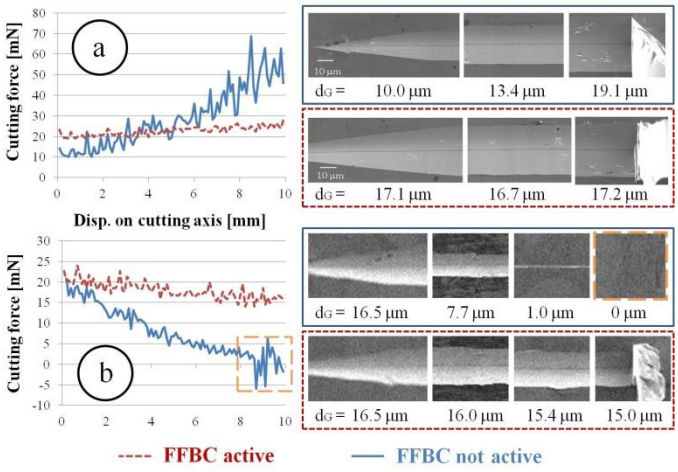

Fig. 6 Cutting experiments on inclined surfaces: (a) positive inclination and (b) negative inclination

Based on the results of previous experiments, it is believed that the fabrication of micro-grooves with constant cutting depth on round surfaces or with more complex topologies is possible. Using this cutting mechanism, only the normal cutting force can be determined.

3. Cutting tool geometry

3.1 Cutting angles in conventional cutting

The geometry and nomenclature of cutting tools, even single-point cutting tools, are surprisingly complicated. It is difficult, for example, to determine the appropriate planes in which the various angles of a single-point cutting tool should be measured [13]. The simplest cutting operation, known as two dimensional or orthogonal cutting, is the one where a straight-edged tool moves with a constant velocity in the direction perpendicular to the cutting edge of the tool (fig. 7a).

Two cutting angles can be observed on this figure: α that represents the rake face angle and γ is the flank (or relief) angle. Some basic definitions that should be introduced are, the **work surface** that is surface of the workpiece that will be removed by machining, the **machined surface** that is the surface produced after the cutting tool pass, the **rake face** that is the surface over which the chip formed during the cutting slides and the **flank face** that is the surface over which the surfaces produced passes. As result of the cutting process, several terms required for the calculation of the cutting forces involved in the manufacturing process are mentioned as well: t_0 is the uncut chip thickness (the thickness of the layer to be removed), w_0 is the uncut chip width, t_C is the chip thickness (layer of material already removed) and w_C is the chip width.

On the other hand, the oblique cutting is shown in fig. 7b. In this type of cutting, the straight cutting edge of the tool is not perpendicular to the direction of the primary motion. The angle which the straight cutting edge makes with the direction of the cutting speed is known as the cutting edge inclination angle λ. The plastic deformation of the layer being removed in the

oblique cutting is more complicated than the one in orthogonal cutting; therefore, oblique cutting cannot be represented as a 2D model [13]. Some of the advantages of oblique cutting are the reduction of the mechanical strength at the tool tip (longer tool life) and, because the chip does not flow along the orthogonal plane, there is less damage in the finished surface.

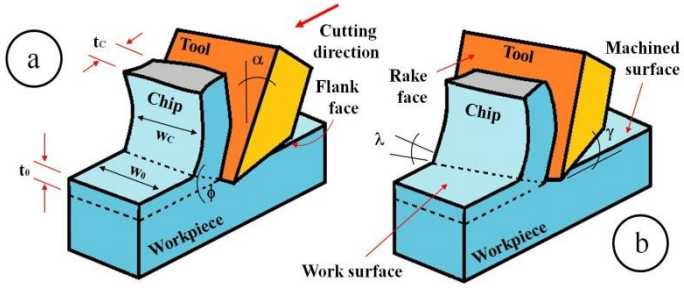

Fig. 7. (a) Orthogonal cutting and (b) oblique cutting

In conventional orthogonal cutting, the rake face angle α is one of the parameters that may affect more significantly the cutting forces. It has been studied [14] that the rake angle is directly related to the shear plane angle (fig. 8) by eq. (1), where the ϕ is the shear plane angle and the r_T is the chip thickness ratio, which can be calculated using eq. (2).

In conventional cutting, it is recommended to use positive rake angles that according to eq. (1) increases the size of the shear plane angle and therefore reduces the shear plane area, which means a lower shear force, obtaining as result lower cutting forces, power and temperature.

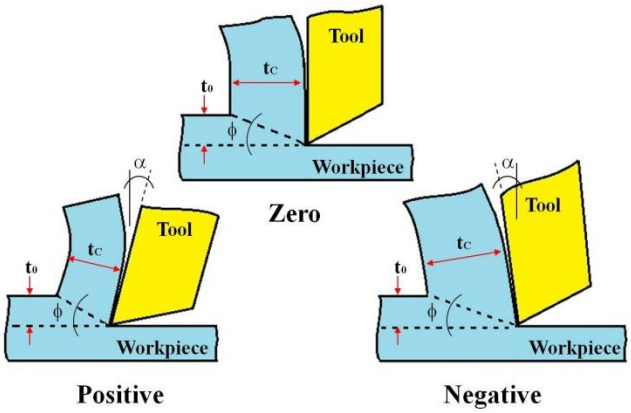

Fig. 8. Relation between the shear plane angle and the rake angle

$$\tan\phi = \frac{r_T \cos\alpha}{1 - r_T \sin\alpha} \quad (1)$$

$$r_T = \frac{t_0}{t_C} \quad (2)$$

3.2 Size effects of micro cutting

When the cutting parameters, such as depth of cut or the uncut chip thickness, are on the same order of amplitude as the tool parameters such as the tool edge radius R, the effective rake angle α_t should be considered, because it may become highly negative. Size effects resulting from the small ratio of uncut chip thickness to the tool edge radius will be a dominant factor for material removal mechanism and chip generation physics in micro cutting [15].

Cutting, ploughing or slipping phenomenon will occur pre-dominated by this ratio, and eventually influences cutting processes such as surface finishing. Figure 9 illustrates the cutting edge radius size effect.

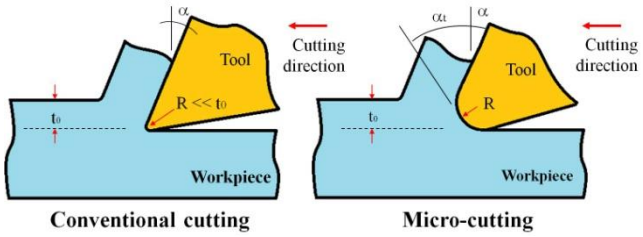

Fig. 9 Size effect of the ratio between the uncut chip thickness and the tool edge radius

On the other hand, when the micro structure of the workpiece material such as grain size is comparable in size to the tool edge radius and depth of cut, the *micro structure size effects* occurs [15]. In micro cutting, the chip formation may take place inside an individual grain, considering that for engineering materials, the grain size varies between few hundreds of nanometers to some tens of micrometers. Therefore, the materials cannot be treated as isotropic and homogeneous like in conventional macro cutting.

3.3 Micro cutting force modelling

The prediction of micro cutting forces is very important for the characterization of the micro cutting mechanism. Nowadays, there are two major approaches to modelling the cutting forces analytically. The first one consists on analyzing the cutting forces on the instantaneous uncut chip cross section, while the second approach is focused on calculating the cutting forces using the shear plane area.

For this study, the conventional basic cutting force model based on the instantaneous uncut chip cross section will be considered. This model is based on the relation shown in eq. (3), where the F_C is the cutting force, k_m is a constant based on the specific cutting energy (energy consumed in removing a unit volume of material) and A is area of the cutting cross section [15-16].

$$F_C = k_m A \quad (3)$$

4. Experimental analysis

4.1 Tool geometry of the CLC mechanism

Some mechanical components were fabricated to vary the tool geometry in the CLC mechanism. Figure 10 shows the mechanism necessary to vary the tool edge inclination angle λ (0° and 15°). Figure 11 shows some of the tool holders fabricated to allow the change of the rake face angle α (0°, -30°,

-15° and 5°). Even different tool holders are used to modify the rake face angle, the contact point is the same for all the cases.

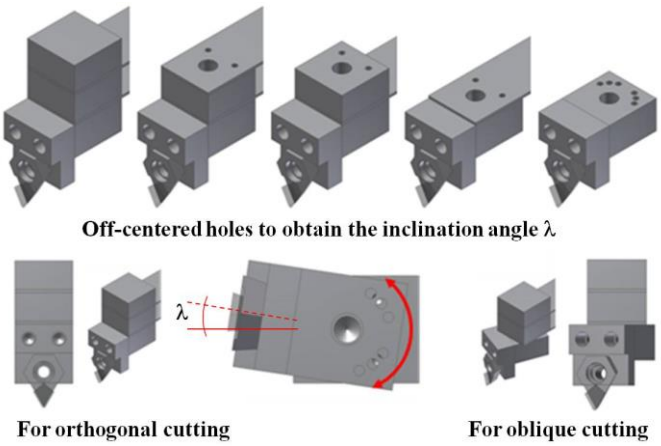

Fig. 10 Mechanism designed to vary the inclination angle λ

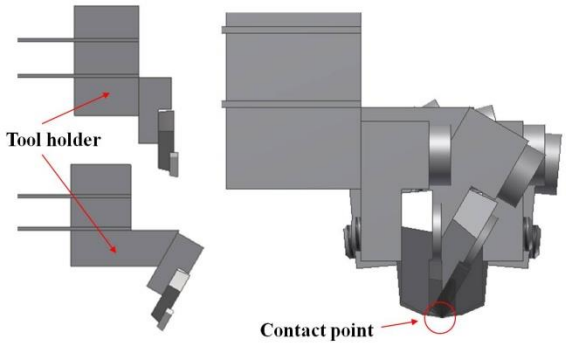

Fig. 11 Tool holders used to vary the rake face angle α

Three single crystal diamond tools with different wedge or cutting angles θ (60°, 90° and 120°) are available for the fabrication of microgrooves with this mechanism. The tool edge radius is in all the cases under 0.10 [μm], and considering that the aim depth of cut is much higher, in the order of couple of micrometers, ploughing effect and elastic recovery can be discarded. The relief angle of the tool γ is approximately 7°. Figure 12 shows the characteristics of the diamond tool used.

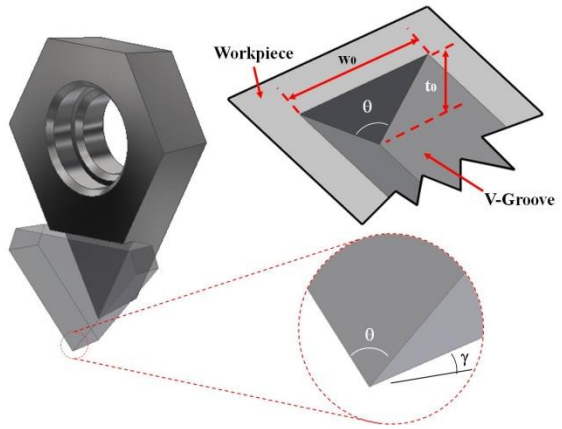

Fig. 12 Characteristics of the single crystal diamond tool

4.2 Cutting experiments using the CLC mechanism

Several cutting experiments were performed to observe, based on the theory described before, how is the behavior of the CLC mechanism during the micro cutting process.

4.2.1 Cutting experiments for oblique and orthogonal cutting

The aim of these cutting experiments is to observe the behavior of the cantilever beam during orthogonal and oblique cuttings. Table 2 shows the cutting conditions for the experiments to be performed in this paper. Table 3 shows the specific cutting conditions for this experiment in particular.

Table 2. Cutting conditions for experiments realized to evaluate the effect of the cutting angle on the CLC mechanism

Workpiece material	Brass (C2801)
Surface inclination	0 [μm/mm]
Tool material	Single crystal diamond
Tool shape	V-shape
Length of the groove	3 [mm]
Initial indentation	5, 10, 15, 20 [μm] (Z axis)
Feed rate	6 [mm/min]
Cutting direction	Front cutting
Others	Dry cutting, FFBC not active

Table 3. Conditions for orthogonal and oblique cuttings

Wedge angle θ	90 [°]
Rake angle α	0 [°]
Inclination angle λ	0 [°], 15 [°]

To compare the orthogonal and oblique cuttings, a simple analysis based on the normal cutting force recorded and the characteristics of the groove fabricated was done. Figure 13 shows a plot that compares the cutting force and the cutting depth of the groove for both experiments. It is possible to observe that for oblique cutting, the recorded cutting force is significantly larger compared to orthogonal cutting experiments. This is because the cross cutting area of the groove is increased significantly for the oblique cutting due to the geometry of the diamond tool. This can be observed in figure 14, where images, obtained using a scanning electron microscope (SEM), shows an upper view of the indentation mark and the fabricated groove.

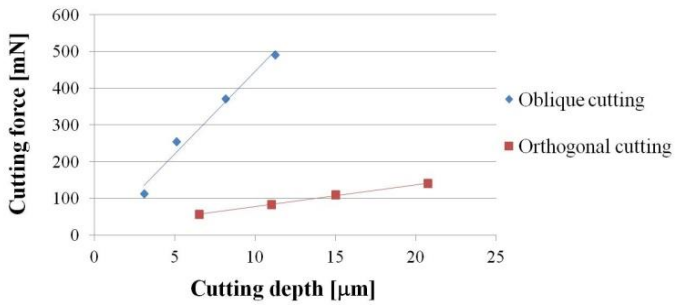

Fig. 13 Normal force vs cutting depth in orthogonal and oblique cutting

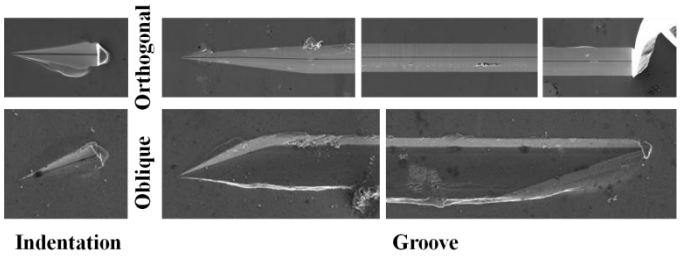

Fig. 14 Indentation marks and grooves fabricated during orthogonal and oblique cuttings

Based on the results obtained, it is not recommended to perform oblique cutting using this mechanism. The cutting force in oblique cutting is much higher compared to the one required for orthogonal cutting; on the other hand, the groove fabricated by oblique cutting presents significant amount of side burr.

4.2.2 Cutting experiments varying the rake face angle α

The second set of experiments are focused on observe the effect of the rake face angle. The cutting conditions for these experiments are shown in table 4. Figure 15 shows the results obtained from the cutting experiment, where the cutting depth is compared to the normal cutting force.

Table 4. Conditions for experiments varying the rake angle

Wedge angle θ	90 [°]
Rake angle α	-30[°], -15[°], 0[°], +5[°]
Inclination angle λ	0 [°]

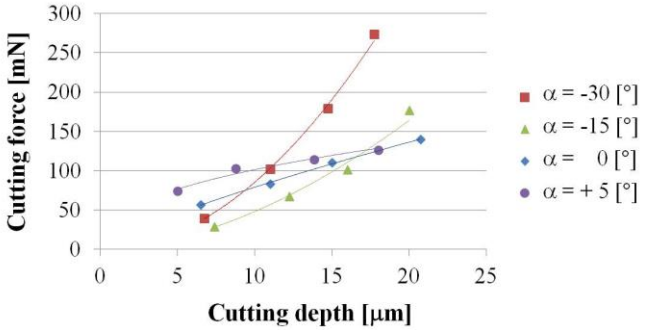

Fig. 15 Normal force vs cutting depth while varying the rake angle

In general terms, when the rake angle has a very negative value (-30 [°]), the cutting forces involved on the cutting process tend to become larger. However, cutting experiments realized in angles between -15 [°] and + 5 [°] seems not to affect signify-cantly the relationship between the force and the depth of cut.

However, in a more detailed analysis of the whole cutting mechanism involved in the machining, it is possible to observe that the rake angle has a more significant effect on the machined surface. The mechanism of cutting for our experiment can be divided in two processes: the indentation and the cutting. The indentation process is done by the Z axis, while the cutting process is realized by the X axis or the Y axis depending on the desired direction of cutting. The LabVIEW interface records the deformation of the cantilever beam for both processes. After the indentation process, when the tool starts to move along the cutting axis, the tip of the cantilever presents a deformation that we called *balance point*, which is the point where the groove reaches its final depth (fig. 16). The figure 17 shows the start and end part of the grooves for each cutting experiment, showing that the more negative is the rake angle, the faster is reached the balance point.

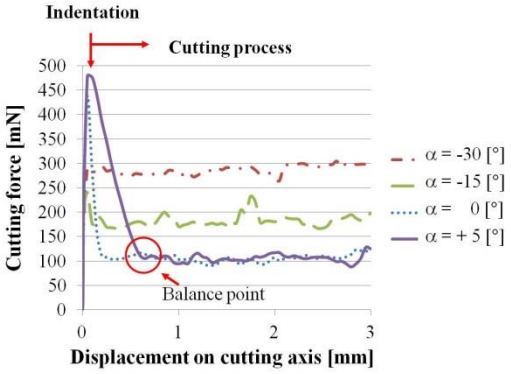

Fig. 16 Balance point observed in the force measurement

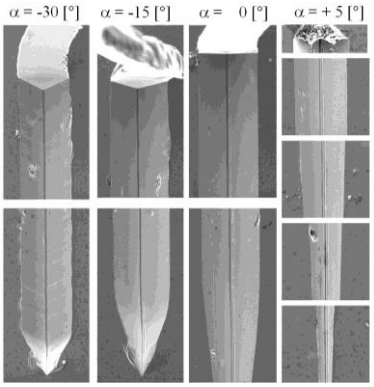

Fig. 17 Fabricated grooves for each rake angle

Using the eqs. (1) and (2), it is possible to estimate the share plane angles ϕ for each case and observe if the effect of the rake face angle in this cutting mechanism is similar to conventional machining. In the fig. 18, it is shown how was measured the cutting width of the groove w_0 and the chip thickness t_C for each cutting experiment, and based on the fig. 12, it is possible to relate the w_0 with the uncut chip thickness t_0 using eq. (4).

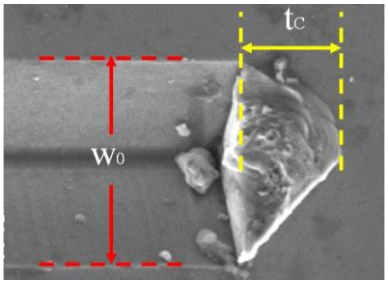

Fig. 18 Measurement of the width of cut and chip thickness

$$d_G = t_0 = \frac{w_0}{2\,tan\left(\frac{\theta}{2}\right)} \quad (4)$$

With this information it was possible to calculate the chip thickness ratio for each experiment, and then using the theoretical rake face angle, the shear plane angle was determined. The results are shown in table 5.

Table 5. Shear plane angles determined on experimental results

Rake angle α [°]	Chip ratio r_T	Shear angle ϕ [°]
-30	1.0432	30.7
-15	0.7205	30.4
0	0.9328	43.01
5	0.9741	46.68

This results confirm that the rake face angle have a similar effect in this mechanism as in conventional cutting; the more positive is the rake face angle, the larger is the shear plane angle, obtaining as result the reduction of cutting forces. However, considering the problem related to the balance point, the use of positive rake angles may not be adequate. On the other hand, even the rake face angle of -30[°] shows a very good response to the balance point, it clearly shows that the cutting forces present on this experiment are higher than the other cases. It is noticeable too on fig. 17, that this experiment is the one that presents an effect similar to vibration in the bottom of the groove. Therefore, based on the results, it is recommended the use of rake face angles between -15 [°] to 0 [°].

4.2.3 Cutting experiments varying the wedge or cutting angle θ

For these experiments, three cutting tools with different cutting angles were used. The cutting conditions are presented in the table 6. In first term, the relationship between the cutting force and the cutting depth of the groove are compared. The results are shown in the plot of the fig. 19, where the normal cutting force is compared with the cutting depth of the groove.

Table 6. Conditions for experiments varying the wedge angle

Wedge angle θ	60 [°], 90 [°], 120 [°]
Rake angle α	0 [°]
Inclination angle λ	0 [°]

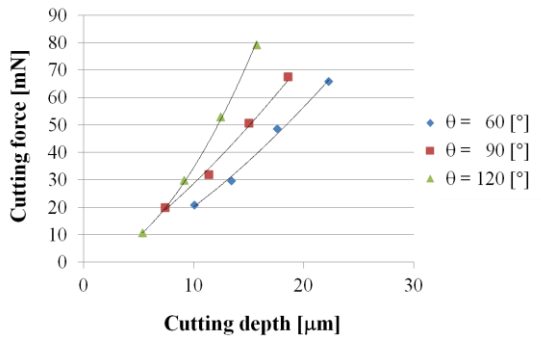

Fig. 19 Cutting force vs cutting depth varying the wedge angle

Based on the results shown in the plot, if the wedge angle is increased, the cutting force involved gets increased as well. This can be predicted based on the model discussed on the section 3.3, considering that the cutting force is directly related to the area of the cutting cross section as shown in eq. (3). In the experimental results shown in figure 19 is possible to observe that the relationship between the cutting depth and the cutting force seems not to be completely linear. In [16], a cutting model based on the eq. (3), that includes a non-linear coefficient is introduced. Equation (5) indicates that the coefficient based on the specific cutting energy is directly related to the chip formation, and it is obtained using the experimental results. Considering the eqs. (3) and (5), it was proposed to apply this cutting model to our CLC mechanism and observe if it is possible to make a first approximation for the modelling of this system. The constants C and n can be obtained from the experimental results presented in fig. 19, using the least squares method.

$$k_m = C{t_C}^{-n} \quad (5)$$

From eqs. (3) and (5), it is possible to deduce eq. (6), which in combination with eq. (4) and using the fig. 12 as reference, it is possible to obtain eq. (7). If eq. (2), is introduced in eq. (7), eq. (8) is derived.

$$F_C = C{t_C}^{-n}A \quad (6)$$

$$F_C = C{t_C}^{-n}{t_0}^2\,tan\left(\frac{\theta}{2}\right) \quad (7)$$

$$F_C = C{r_T}^n\,tan\left(\frac{\theta}{2}\right){t_0}^{2-n} \quad (8)$$

The model presented on eq. (8) is based on the geometry of the cutting depth and the wedge angle of the diamond tools used. The chip thickness ratio was obtained based on the cutting experiments realized, and are presented on table 7.

Table 7. Chip thickness ratio obtained from cutting experiments

Wedge angle θ	Chip ratio r_T
60 [°]	0.6319
90 [°]	0.518
120 [°]	0.4324

Using as reference the results obtained from the experiment of the 90 [°] tool it was possible to determine the experimental constants C and n, which are 1.9399 and 0.6461 respectively.

To observe if the model can be applicable to our mechanism, the theoretical results will be compared with the experimental results already obtained for the diamond tools of 60 and 120 [°].

As it is possible to observe in fig. 20, in both cases the cutting model can be used to make a good estimation of the cutting force compared to the cutting depth. This is a first step to achieve a more reliable cutting model for our cutting mechanism.

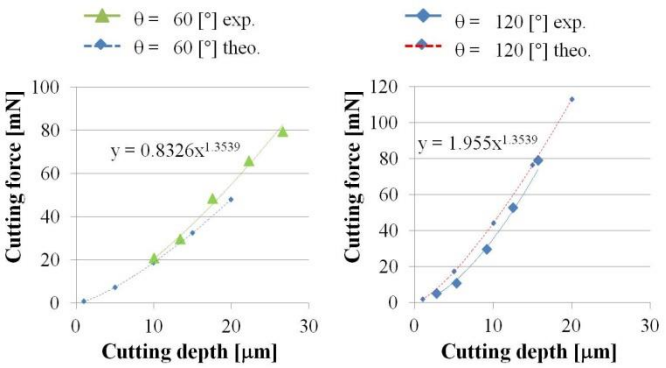

Fig. 20 Comparison between experimental results and analytical cutting force model

In the case of the wedge angle variation, there is no restriction in the use of any of the cutting tools. With the experimental results obtained, it was possible to obtain a simple model based on the specific cutting energy that can give a good approximation of the cutting forces involved in the fabrication of micro-grooves.

5. Conclusions

A new cutting mechanism was developed for the fabrication of micro-grooves. Its operation principle is based on the nano-cutting machining technique using an atomic force microscope. In this mechanism, the tool is mounted on a cantilever beam, which during the cutting process undergoes a deformation that is necessary to implement a force feedback control system. Due to the fact that the cantilever beam is a non-rigid body, it is necessary to study how the cutting forces affect its deformation. The aim of this study was to analyze the effect of the tool geometry on the deformation of the cantilever. Three main cutting angles were analyzed: the inclination angle, the rake face angle and the wedge or cutting angle. From the analysis, it is possible to conclude the following:

- Thus it is possible to perform orthogonal cutting and oblique cutting, it is not recommended to perform the oblique cutting because the cutting force resultant from the experiment is much higher in comparison to the orthogonal cutting, and there is not seen any other advantage from the oblique cutting.
- The rake face angle has a similar effect in this mechanism as in conventional cutting. However, due to the deformation of the cantilever, it is recommended the use of rake face angles between -15[°] and 0 [°]. More negative angles present a large cutting force and vibration in the workpiece, while positive angles show an unstable state to reach the aim cutting depth.
- In the case of the wedge angle, there is no restriction for the use of any tool available. During this analysis a basic cutting model was proposed to estimate the cutting force in the manufacturing process.

ACKNOWLEDGEMENT

This study was supported by the Japan Society for the Promotion of Science KAKENHI Grant Number 26289022. Its support is gratefully acknowledged.

REFERENCES

1. Biddut A.Q., Rahman M., Neo K. S., Rezaur Rahman K. M., Sawa M., Maeda Y. Performance of single crystal diamond tools with different rake angles during micro-grooving on electrodes nickel plated die materials. Intl. J. of Adv. Manuf. Tech., Vol. 33 (2007) 891-899.
2. Lee J. M., Je T. J., Choi D. S., Lee S. W., Le D., Kim S. J. Micro grooving simulation and optimization in the roughing stage. Intl. J. of Precision Engineering and Manufacturing, Vol. 11 (2010) No. 3, pp. 361-368.
3. Kim G. D., Loh B. G. Machining of micro-channels and pyramidal patterns using elliptical vibration cutting. Intl. J. of Advanced Manufacturing Technology, Vol. 49 (2010), pp. 961-968.
4. Yan J., Zhang Z., Kuriyagawa T. Fabricating micro-structured surface by using single-crystalline diamond endmill. Int. J. Manuf. Technol., Vol. 51 (2010), pp. 957-964.
5. Moriya T., Nakamoto K., Ishida T., Takeuchi Y. Creation of V-shaped microgrooves with flat-ends by 6-axis control ultraprecision machining. CIRP Annals, Manufacturing Technology, Vol. 59 (2010), pp. 61-66.
6. Ashida K., Herrera G., Ogura I., Okazaki Y. Basic study of micro-groove cutting using an elastic leaf spring type tool holder. Intl. Conference on MicroManufacturing, ICOMM (2011).
7. Herrera-Granados G., Ashida K., Ogura I., Okazaki Y., Morita N. Ruiz-Huerta L., Caballero-Ruiz A. Micro-groove cutting for different materials using an elastic leaf spring type tool holder. Key Engineering Materials 523-524 (2012), pp. 93-98
8. Yan Y., Sun T., Liang Y., Dons S. Investigation on AFM-based micro/nano CNC machining system. Intl. Journal of Machine Tools and Manufacture 47 (2007), pp. 1651-1659
9. Ashida K., Morita N., Yoshida Y. Study on Nano-Machining Process Using Mechanism of a Friction Force Microscope. JSME Int. J., Series C, 44-1 (2001), pp. 244-253
10. Kawasegi N., Takano N., Oka D., Morita N., Yamada S., Kanda K., Takano S., Obata T., Ashida K. Nanomachining of Silicon Surface Using Atomic Force Microscope With Diamond Tip. J. Manuf. Sci. Eng. (2006) Vol. 128, Issue 3, pp. 723-729.
11. Lee S. H. Analysis of ductile mode and brittle transition of AFM nanomachining of silicon. Intl. J. of Machine Tools and Manufacture, Vol. 61 (2012), 71-79.
12. Herrera-Granados G., Ashida K., Ogura I., Okazaki Y., Morita N., Hidai H., Matsusaka S. Basic study on micro/nano-scale cutting applying machining force control system. Japan Society for Precision Engineering, Spring meeting. JSPE (2013).
13. Astakhov V. Tribology of metal cutting, appendix A. Tribology and Interface Engineering Series, No. 52. Elsevier Science, 2006.
14. Merchant E. Metalc Cutting Process I. Orthogonal Cutting and a Type 2 Chip. Journal of Applied Physics, Vol. 16 (1945), Number 5.
15. Cheng K., Huo D. Micro-cutting. Fundamentals and Applications. Wiley, 2013.
16. Lee J. M., Je T. J., Choi D. S., Lee S. W., Le D., Kim S. J. Micro Grooving Simulation and Optimization in the Roughing Stage. Intl. J. of Precision Eng. and Manuf. Vol. 11 (2010) No. 3, pp. 361-368.